Journal of Applied Mechanics and Technical Physics, Vol. 47, No. 4, pp. 461–471, 2006

MOVEMENT OF THE GROUND IN RAYLEIGH WAVES PRODUCED BY UNDERGROUND EXPLOSIONS

V. A. Simonenko. N. I. Shishkin, and G. A. Shishkina

UDC 550.348.425.4

Analytic representations are obtained for the displacement and stress fields in the Rayleigh surface wave (R-wave) generated in an elastic half-space by an internal source that produces the same seismic P-wave as an underground explosion. Oscillograms, particle trajectories, and stresses in the half-space and on its surface are calculated. Relations for the energy flux in the R-wave are obtained. For rock salt, the fraction of the explosion energy transferred to the R-wave is estimated. It is established that this fraction can reach values of about 1% of the total explosion energy if the explosion is a contained one. As the charge depth is increased, the energy of the R-wave decreases in approximately inverse proportion to the depth.

Key words: *underground explosion, Rayleigh wave, displacement, stress, energy flux.*

Introduction. Elastic surface Rayleigh waves (R-waves) [1] result from dynamic actions on the surface of elastic bodies. In structures of small dimensions, they are used as ultrasonic waves. Rayleigh waves are also observed in large structures and engineering constructions. In addition, R-waves are produced by explosions, earthquakes, and impacts of cosmic bodies on the planets. Seismic R-waves are used to probe the Earth's crust and to study its structure, and long R-waves are used to study the Earth's mantle. Rayleigh waves produced by explosions contain a significant fraction of the explosion energy, and at a certain distance from the epicenter, they dominate the other seismic waves. They contain information on the energy source and the properties of the medium. For example, records of R-waves from some underground nuclear explosions suggest that spall fracture of the medium occurs at the epicenters of the explosions [2]. In [3], it is shown that during impacts of cosmic bodies on the Earth, the focusing of R-waves in the antipode region (the region opposite to the site of impact) can lead to the formation of unusual geological structures such as explosion pipes or diatremes.

Rayleigh waves produced by a point source in an elastic half-space were considered in [4–6]. Petrashen' [7] studied the Lamb problem for the case of an isotropic elastic sphere and obtained expressions for Rayleigh waves on the surface of an elastic sphere. Onis'ko and Shemyakin [8] studied the movement of the ground surface for an explosion in a half-space, and Alterman and Abramovici [9] explored the movement of the surface of an elastic sphere for a contained explosion. Brekhovskikh [10] investigated Rayleigh waves produced by a harmonious source and propagating along the curved surface of an elastic body. The present paper gives more detailed results for Rayleigh waves on both the surface of an elastic half-space and inside it for explosions at a great depth. The energy flux transferred by the Rayleigh wave is considered, and the fraction of the explosion energy converted into the R-wave energy is estimated. Such data are required to obtain more exact estimates of the damage to various engineering constructions from R-waves and describe the dynamic geological processes occurring in the regions that are diametrically opposite to the site of impact of cosmic bodies on the surface of the planets [3].

Institute of Technical Physics, Snezhinsk 456770; simonenko@vniitf.ru. Translated from Prikladnaya Mekhanika i Tekhnicheskaya Fizika, Vol. 47, No. 4, pp. 3–14, July–August, 2006. Original article submitted June 29, 2005.

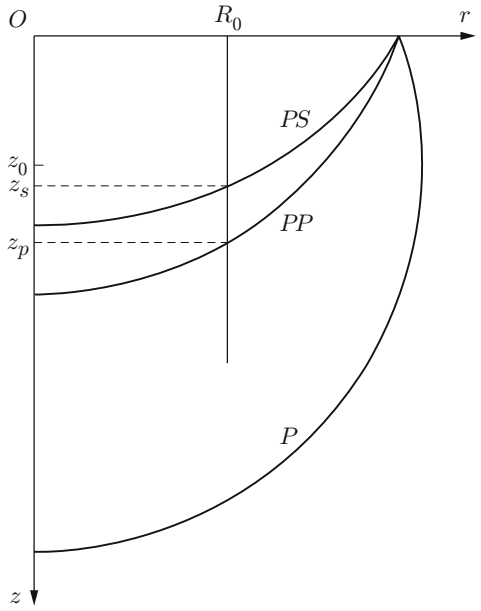

Fig. 1. Coordinate system, the positions of the wave fronts, and the control surface (a cylinder of radius R_0).

1. Wave Source. The seismic longitudinal P-wave produced by an underground nuclear explosion is described in [11] using the elastic-displacement field potential containing three free parameters:

$$\varphi(t, R) = -\frac{\Phi(\infty)}{R}\, f(\tau). \tag{1.1}$$

Here $t \geqslant 0$ is the time reckoned from the moment of the explosion, $R > 0$ is the distance to the center of the explosion, $\Phi(\infty)f(\tau)$ is the reduced potential, $\Phi(\infty)$ is the stationary value of the reduced potential, $f(\tau) = 1 - \mathrm{e}^{-\tau}(1 + \tau + \tau^2/2 + \tau^3/6 - B\tau^4)$ is a function of the source that produces the same seismic P-wave as the underground explosion, $\tau = (t - R/c_p)/t_0$ (t_0 is the characteristic duration of wave generation and c_p is the propagation velocity of the longitudinal elastic waves), and B is a constant that depends on the properties of the medium. The characteristic time t_0 is related to the characteristic length $c_p t_0$, which for rock is approximately equal to the radius of the crushing zone around the center of the explosion.

It should be noted that the approximating fourth-order polynomial contained in the source function provides a satisfactory description of the potential in the near seismic region of the explosion. As shown in [12], at teleseismic distances, the second-order polynomial is a more adequate approximation. In addition, for explosions at shallow depths, at which spalling occurs at the explosion epicenter, the third-order polynomial [2] is more suitable. These approximations can be obtained by discarding the corresponding terms of the polynomial and by selecting the coefficient B for the higher-order term of the polynomial in the function $f(\tau)$. The energy E_p radiated to "infinity" in the form of P-waves is defined by the formula [11]

$$E_p = \pi\alpha(B)\rho_0 c_p^2 \varkappa \Phi(\infty), \tag{1.2}$$

where ρ_0 is the density of the medium, $\alpha(B) = (5 + 3(1 + 24B)^2)/64$, and $\varkappa = \Phi(\infty)/(c_p t_0)^3$.

2. Rayleigh Wave. A point-source explosion in a homogeneous elastic medium generates a longitudinal-type seismic wave (P-wave). The interaction of this wave with the free surface produces a surface seismic wave or a Rayleigh wave.

Let us consider the movement that occurs in an elastic half-space subjected to the action of the source (1.1). We introduce cylindrical coordinates $Or\varphi z$ with the axis z directed into the interior of the medium and the axis r along the free surface $z = 0$ (Fig. 1). The source is placed at the point $(0, z_0)$. The movement is assumed to be

independent of the angular coordinate φ. From the initial time $t = 0$ to the moment the P-wave approaches the free surface, the movement is described by the potential (1.1), which in dimensionless variables is written as

$$\varphi_0(t, r, z) = -f(t - \sqrt{r^2 + (z_0 - z)^2}\,)/\sqrt{r^2 + (z_0 - z)^2}\,. \tag{2.1}$$

Here the time t is in units of t_0 and the distance is in units of $c_p t_0$. The potential (2.1) can be written as

$$\varphi_0(t, r, z) = \varphi(t, R)/(\varkappa (c_p t_0)^2), \qquad R = \sqrt{r^2 + (z_0 - z)^2}\,.$$

From the time of the beginning of reflection of the P-waves from the free surface, the movement is described by the potentials φ_1 and $\boldsymbol{\psi}(0, \psi, 0)$, which are linked to the displacement field $\boldsymbol{u}$ by the relation

$$\boldsymbol{u} = \operatorname{grad} \varphi_1 + \operatorname{rot} \boldsymbol{\psi},$$

where $\varphi_1 = \varphi_0 + \varphi$. The potentials φ and ψ are found by solving the wave equations of elasticity theory

$$\frac{\partial^2 \varphi}{\partial t^2} = \Delta \varphi, \qquad \frac{1}{\gamma^2}\,\frac{\partial^2 \psi}{\partial t^2} = \Delta \psi - \frac{\psi}{r^2}, \qquad t \geqslant z_0, \quad r \geqslant 0, \quad z \geqslant 0 \tag{2.2}$$

(Δ is the Laplacian and $\gamma = c_s/c_p$, where c_s is the propagation velocity of the shear waves) for zero initial data and zero stress vector on the free surface:

$$\varphi\Big|_{t=0} = \psi\Big|_{t=0} = \frac{\partial \varphi}{\partial t}\Big|_{t=0} = \frac{\partial \psi}{\partial t}\Big|_{t=0} = 0,$$

$$\Big[\Big(\frac{1}{\gamma^2} - 2\Big)\frac{\partial^2 \varphi}{\partial t^2} + 2\,\frac{\partial^2 \varphi}{\partial z^2} + 2\,\frac{\partial^2 \psi}{\partial r \partial z} + \frac{2}{r}\,\frac{\partial \psi}{\partial r}\Big]\Big|_{z=0} = -\Big[\Big(\frac{1}{\gamma^2} - 2\Big)\frac{\partial^2 \varphi_0}{\partial t^2} + 2\,\frac{\partial^2 \varphi_0}{\partial z^2}\Big]\Big|_{z=0}, \tag{2.3}$$

$$\Big(2\,\frac{\partial^2 \varphi}{\partial r\,\partial z} + \frac{1}{\gamma^2}\,\frac{\partial^2 \psi}{\partial t^2} - 2\,\frac{\partial^2 \psi}{\partial z^2}\Big)\Big|_{z=0} = -2\,\frac{\partial^2 \varphi_0}{\partial r\,\partial z}\Big|_{z=0}.$$

Applying the Laplace transform with respect to t and the Fourier–Bessel transform with respect to r, we obtain a solution of the problem (2.2), (2.3) in the form [6, 13]

$$\varphi(t, r, z) = \varphi_0(t, r, z_1) - \varphi_0(t, r, z_2) + \varphi_1(t, r, z_2),$$

$$\varphi_0(t, r, z) = -f(t - \rho)/\rho, \qquad \rho = (r^2 + z^2)^{1/2}, \qquad z_1 = z - z_0, \qquad z_2 = z + z_0,$$

$$\varphi_1(t, r, z_2) = \gamma \int_0^\infty k J_0(kr)\Big[\frac{1}{2\pi i}\int_l F(k\gamma\xi) X(\xi)\, \mathrm{e}^{-k g_1(\xi)}\, d\xi\Big]\, dk, \tag{2.4}$$

$$\psi(t, r, z_2) = \gamma \int_0^\infty k J_1(kr)\Big[\frac{1}{2\pi i}\int_l F(k\gamma\xi) Y(\xi)\, \mathrm{e}^{-k g_2(\xi)}\, d\xi\Big]\, dk,$$

where

$$X(\xi) = 8\beta/(\delta^2 - 4\alpha\beta), \quad Y(\xi) = 4\delta/(\delta^2 - 4\alpha\beta), \quad g_1(\xi) = \alpha z_2 - \gamma\xi t, \quad g_2(\xi) = \alpha z_0 + \beta z - \gamma\xi t,$$

$$\alpha = (1 + \gamma^2\xi^2)^{1/2}, \quad \beta = (1 + \xi^2)^{1/2}, \quad \delta = 2 + \xi^2, \quad \operatorname{Re}\alpha > 0, \quad \operatorname{Re}\beta > 0 \quad \text{for } \xi > 0,$$

$F(k\gamma\xi)$ is the Laplace image of the source function $f(t)$, J_0 and J_1 are Bessel functions, and l is the integration contour in the Laplace transform inversion formula.

In (2.4), the integrands have the following singularities on the plane of the complex variable ξ: 1) the branching points $\xi_{1,2} = \pm i/\gamma$ and $\xi_{3,4} = \pm i$; 2) the pole $\xi = 0$; 3) the possible singularities of the function $F(k\gamma\xi)$; 4) the poles $\xi_R = \pm i\theta$ $[0.874 \leqslant \theta(\gamma) \leqslant 0.955]$.

The poles ξ_R are solutions of the Rayleigh equation $\delta^2 - 4\alpha\delta = 0$. Each singularity defines the corresponding term in the general solution of the problem (2.2), (2.3). The branching points correspond to body waves. The pole at the coordinate defines the asymptotics of the solution as $t \to \infty$, and the Rayleigh poles define the surface wave as the asymptotics for $r \gg c_p t_0$ and $t > t_s$ (t_s is the time of the shear wave arrives at the point considered).

In the present paper, we study the motion in Rayleigh waves that is described by the formulas obtained from (2.4) by finding the residues at the Rayleigh poles with subsequent integration over the parameter k. The displacements, displacement rates, and stresses are expressed in terms of the potentials φ and ψ by the well-known formulas of elasticity theory. The expressions for the displacements, displacement rates, and stresses in the Rayleigh wave are given below.

The displacements are given by

$$\boldsymbol{u} = u_r \boldsymbol{r}_1 + u_z \boldsymbol{z}_1,$$

$$\boldsymbol{u}(t,r,z) = \int\limits_0^{t-t_p} \boldsymbol{U}^p(t-\tau,r,z) f''(\tau)\,d\tau + \int\limits_0^{t-t_s} \boldsymbol{U}^s(t-\tau,r,z) f''(\tau)\,d\tau,$$

$$\boldsymbol{U}^p = U_r^p \boldsymbol{r}_1 + U_z^p \boldsymbol{z}_1, \qquad \boldsymbol{U}^s = U_r^s \boldsymbol{r}_1 + U_z^s \boldsymbol{z}_1, \tag{2.5}$$

$$U_r^p = \frac{4ab^2}{\gamma\theta^3\Theta}\, S_{10}(r, az_2, \gamma\theta t)\varepsilon(t-t_p), \qquad U_r^s = -\frac{2ab^2 d}{\gamma\theta^3\Theta}\, S_{10}(r, az_0+bz, \gamma\theta t)\varepsilon(t-t_s),$$

$$U_z^p = \frac{4a^2b^2}{\gamma\theta^3\Theta}\, S_{00}(r, az_2, \gamma\theta t)\varepsilon(t-t_p), \qquad U_z^s = -\frac{2abd}{\gamma\theta^3\Theta}\, S_{00}(r, az_0+bz, \gamma\theta t)\varepsilon(t-t_s),$$

where $\boldsymbol{r}_1$ and $\boldsymbol{z}_1$ are unit vectors of the coordinate system, $f''(\tau)$ is the second derivative of the source function, and $\varepsilon(x) = 1$ at $x \geqslant 0$ or $\varepsilon(x) = 0$ at $x < 0$.

The displacement rates are given by

$$\boldsymbol{v} = v_r \boldsymbol{r}_1 + v_z \boldsymbol{z}_1,$$

$$\boldsymbol{v}(t,r,z) = \int\limits_0^{t-t_p} \boldsymbol{V}^p(t-\tau,r,z) f''(\tau)\,d\tau + \int\limits_0^{t-t_s} \boldsymbol{V}^s(t-\tau,r,z) f''(\tau)\,d\tau,$$

$$\boldsymbol{V}^p = V_r^p \boldsymbol{r}_1 + V_z^p \boldsymbol{z}_1, \qquad \boldsymbol{V}^s = V_r^s \boldsymbol{r}_1 + V_z^s \boldsymbol{z}_1, \tag{2.6}$$

$$V_r^p = \frac{4ab^2}{\theta^2\Theta}\, C_{11}(r, az_2, \gamma\theta t)\varepsilon(t-t_p), \qquad V_r^s = -\frac{2ab^2 d}{\theta^2\Theta}\, C_{11}(r, az_0+bz, \gamma\theta t)\varepsilon(t-t_s),$$

$$V_z^p = \frac{4a^2b^2}{\theta^2\Theta}\, C_{01}(r, az_2, \gamma\theta t), \varepsilon(t-t_p), \qquad V_z^s = -\frac{2abd}{\theta^2\Theta}\, C_{01}(r, az_0+bz, \gamma\theta t)\varepsilon(t-t_s).$$

In (2.5) and (2.6), the following notation is used: $a^2 = 1-\gamma^2\theta^2$, $b^2 = 1-\theta^2$, $d = 2-\theta^2$, $\Theta = abd-(a^2+\gamma^2 b^2)$, $\theta(\gamma)$ is a solution of the Rayleigh equation $d^2 - 4ab = 0$, $t_p = \sqrt{r^2+(z_0+z)^2}$, and t_s are the times of arrival of the reflected longitudinal and shear waves at the examined point of the medium. The value of t_s can be found from the relation

$$t_s = \sqrt{z_0^2 + C^2} + \sqrt{(r-C)^2 + z^2}/\gamma, \tag{2.7}$$

where C is a positive solution of the equation

$$(r-C)\sqrt{z_0^2+C^2} - \gamma C\sqrt{(r-C)^2+z^2} = 0, \tag{2.8}$$

which is found by iterations:

$$C \approx C_n = r(1-\alpha_n) \qquad (n = 0, 1, 2, \ldots),$$

$$\alpha_0 = 0, \quad \alpha_1 = \frac{\gamma z}{(r^2+z_0^2+z^2)^{1/2}}, \quad \ldots, \quad \alpha_n = \frac{\gamma(1-\alpha_{n-1})(\alpha_{n-1}^2 r^2 + z^2)^{1/2}}{[(1-\alpha_{n-1})^2 r^2 + z_0^2 + z^2]^{1/2}}.$$

The stress tensor has the following nonzero components: σ_{rr}, $\sigma_{rz}=\sigma_{zr}$, $\sigma_{\varphi\varphi}$, and σ_{zz}, where $\sigma_{ik}=\sigma_{ik}^{\varphi}+\sigma_{ik}^{\psi}$ $(i=r,\varphi,z;\ k=r,\varphi,z)$; σ_{ik}^{φ} and σ_{ik}^{ψ} are terms due to the potentials φ and ψ, respectively:

$$\sigma_{rr}^{\varphi}=\int\limits_0^{t-t_p}\Sigma_{rr}^{\varphi}(t-\tau,r,z)f''(\tau)\,d\tau,\qquad \sigma_{rr}^{\psi}=\int\limits_0^{t-t_s}\Sigma_{rr}^{\psi}(t-\tau,r,z)f''(\tau)\,d\tau,$$

$$\sigma_{rz}^{\varphi}=\int\limits_0^{t-t_p}\Sigma_{rz}^{\varphi}(t-\tau,r,z)f'''(\tau)\,d\tau,\qquad \sigma_{rz}^{\psi}=\int\limits_0^{t-t_s}\Sigma_{rz}^{\psi}(t-\tau,r,z)f'''(\tau)\,d\tau.$$

Here $f'''(\tau)$ is the third derivative of the source function, and

$$\Sigma_{rr}^{\varphi}=\frac{8\gamma ab^2}{\theta^3\Theta}\Big(\frac{2a^2+\theta^2}{2}\,S_{01}(r,az_2,t\gamma\theta)-\frac{1}{r}\,S_{10}(r,az_2,t\gamma\theta)\Big)\varepsilon(t-t_p),$$

$$\Sigma_{rr}^{\psi}=-\frac{4\gamma ab^2d}{\theta^3\Theta}\Big(S_{01}(r,az_0+bz,t\gamma\theta)-\frac{1}{r}\,S_{10}(r,az_0+bz,t\gamma\theta)\Big)\varepsilon(t-t_s),$$

$$\Sigma_{\varphi\varphi}^{\varphi}=\frac{8\gamma ab^2}{\theta^3\Theta}\Big(\frac{1-2\gamma^2}{2\gamma^2}\,\theta^2S_{01}(r,az_2,t\gamma\theta)+\frac{1}{r}\,S_{10}(r,az_2,t\gamma\theta)\Big)\varepsilon(t-t_p),$$

$$\Sigma_{\varphi\varphi}^{\psi}=-\frac{4\gamma ab^2d}{\theta^3\Theta r}\,S_{10}(r,az_0+bz,t\gamma\theta)\varepsilon(t-t_s),$$

$$\Sigma_{zz}^{\varphi}=-\frac{4\gamma ab^2d}{\theta^3\Theta}\,S_{01}(r,az_2,t\gamma\theta)\varepsilon(t-t_p),\qquad \Sigma_{zz}^{\psi}=\frac{4\gamma ab^2d}{\theta^3\Theta}\,S_{01}(r,az_0+bz,t\gamma\theta)\varepsilon(t-t_s),$$

$$\Sigma_{rz}^{\varphi}=-\frac{8\gamma a^2b^2}{\theta^3\Theta}\,S_{11}(r,az_2,t\gamma\theta)\varepsilon(t-t_p),\qquad \Sigma_{rz}^{\psi}=\frac{2\gamma abd^2}{\theta^3\Theta}\,S_{11}(r,az_0+bz,t\gamma\theta)\varepsilon(t-t_s).$$

$$\Sigma_{rr}^{\varphi}=\frac{8\gamma ab^2}{\theta^3\Theta}\Big(\frac{2a^2+\theta^2}{2}\,S_{01}(r,az_2,t\gamma\theta)-\frac{1}{r}\,S_{10}(r,az_2,t\gamma\theta)\Big)\varepsilon(t-t_p),$$

$$\Sigma_{rr}^{\psi}=-\frac{4\gamma ab^2d}{\theta^3\Theta}\Big(S_{01}(r,az_0+bz,t\gamma\theta)-\frac{1}{r}\,S_{10}(r,az_0+bz,t\gamma\theta)\Big)\varepsilon(t-t_s),$$

$$\Sigma_{\varphi\varphi}^{\varphi}=\frac{8\gamma ab^2}{\theta^3\Theta}\Big(\frac{1-2\gamma^2}{2\gamma^2}\,\theta^2S_{01}(r,az_2,t\gamma\theta)+\frac{1}{r}\,S_{10}(r,az_2,t\gamma\theta)\Big)\varepsilon(t-t_p),$$

$$\Sigma_{\varphi\varphi}^{\psi}=-\frac{4\gamma ab^2d}{\theta^3\Theta r}\,S_{10}(r,az_0+bz,t\gamma\theta)\varepsilon(t-t_s),$$

$$\Sigma_{zz}^{\varphi}=-\frac{4\gamma ab^2d}{\theta^3\Theta}\,S_{01}(r,az_2,t\gamma\theta)\varepsilon(t-t_p),\qquad \Sigma_{zz}^{\psi}=\frac{4\gamma ab^2d}{\theta^3\Theta}\,S_{01}(r,az_0+bz,t\gamma\theta)\varepsilon(t-t_s),$$

$$\Sigma_{rz}^{\varphi}=-\frac{8\gamma a^2b^2}{\theta^3\Theta}\,S_{11}(r,az_2,t\gamma\theta)\varepsilon(t-t_p),\qquad \Sigma_{rz}^{\psi}=\frac{2\gamma abd^2}{\theta^3\Theta}\,S_{11}(r,az_0+bz,t\gamma\theta)\varepsilon(t-t_s).$$

The functions $C_{mn}(r,p,q)$ and $S_{mn}(r,p,q)$ of three arguments are the real and imaginary parts of the known integrals

$$C_{mn}(r,p,q)+iS_{mn}(r,p,q)=\int\limits_0^{\infty}J_m(kr)\,\mathrm{e}^{-k(p-iq)}\,k^n\,dk\qquad (m=0,1,\quad n=0,1),$$

TABLE 1

Explosion	q, kton	h, m	ρ_0, kg/m^3	c_p, m/sec	$\Phi(\infty)$, m^3	B	$\Phi_1(\infty)$, m^3/kton	c_pt_0, m/kton$^{1/3}$	z_0	η, %
1	2	3	4	5	6	7	8	9	10	11
Gnome	3.1 [15]	360 [16]	2200 [11]	4080 [11]	3120 [17] 2740 [11]	0.17 [11]	1040 895	82	4.4	7.0 6.0
Salmon	5.3 [18]	828 [18]	2240 [15]	4670 [19]	3700 [18, 19] 3770 [14]	0.06 [14]	700 719	57	14.4	3.2 3.3

which are expressed explicitly as

$$C_{00}(r,p,q) = M/R, \qquad S_{00}(r,p,q) = N/R,$$

$$C_{01}(r,p,q) = (p(XM - YN) + q(XN + YM))/R^3,$$

$$S_{01}(r,p,q) = (p(XN + YM) - q(XM - YN))/R^3,$$

$$C_{11}(r,p,q) = r(XM - YN)/R^3, \qquad S_{11}(r,p,q) = r(XN + YM)/R^3,$$

$$C_{10}(r,p,q) = (R - pM - qN)/(rR), \qquad S_{10}(r,p,q) = (qM - pN)/(rR),$$

$$M^2 = (R + |X|)/2, \quad N^2 = (R - |X|)/2, \quad R^2 = X^2 + Y^2, \quad X = r^2 + p^2 - q^2, \quad Y = 2qp.$$

3. Calculations of Motion in the *R*-wave. The motion in the R-wave is localized in a surface layer of the medium whose thickness is on the order of the wavelength λ, from which the range of z is determined to be $0 \leqslant z \leqslant \lambda$. As shown in [9], the R-wave length is close to the length of the P-wave generated by the source. From formula (1.1) it follows that the dimensionless length of the P-wave is $\lambda \approx 10$.

The displacements, displacement rates, and stresses in the medium due to R-wave propagation were calculated for explosions in rock salt since for this rock we know the parameters of the function of an elastic source that forms the same P-wave as an underground explosion. The source parameters $\Phi(\infty)$, c_pt_0, and B were calculated in [11, 14] from the data of the Gnome (1961) and Salmon (1964) U.S. explosion tests. The initial data on the explosion, the parameters of the medium, and seismic processes are given in columns 2–7 of Table 1. In column 2, the explosion energy q is in kilotons of TNT equivalent, as is adopted in the papers cited (1 kton $= 4.18 \cdot 10^{12}$ J), and the charge depth h is in meters. According to these data, the value of the parameter γ for rock salt is about 0.6. Column 8 gives the values of the potential $\Phi_1(\infty)$ obtained using the data of columns 2, 3, and 6, column 9 gives the characteristic scale c_pt_0, column 10 the relative depth of the explosion z_0, and column 11 the explosion energy $\eta = E_p/E_0$ converted to the P-wave energy obtained from the data of column 6 (E_0 the total explosion energy).

Thus, the source parameters and the amount of energy transferred to the P-wave depend on the charge depth. This is obviously due to the effect of lithostatic pressure.

3.1. *Displacements.* Figure 2 gives curves of the displacement versus time at the points located at various reduced depths $0 \leqslant \bar{z} \leqslant 10$ [$\bar{z} = z/(c_pt_0)$]. The amplitude of the horizontal component u_r has the largest value on the free surface $\bar{z} = 0$. As the depth increases, it decreases linearly and changes sign at $\bar{z} = z_s$. With a further increase in the depth, the amplitude increases in the absolute value, reaches a maximum at a certain depth, and then decreases monotonically. The surface $\bar{z} = z_s$ is at approximately the same level as in the case of a harmonic R-wave of the same length:

$$z_s \approx -\frac{1}{4\pi}\,\frac{\ln\left(\sqrt{1-\gamma^2\theta^2}\sqrt{1-\theta^2}\right)}{\sqrt{1-\gamma^2\theta^2} - \sqrt{1-\theta^2}}. \tag{3.1}$$

For all possible values of $\gamma \in (0, 1/\sqrt{2})$, the boundary z_s is in the interval $0.135 \leqslant z_s \leqslant 0.250$.

At the depth increases, the amplitude of the vertical displacement component u_z first increases weakly, reaches a certain maximum, and then decreases almost exponentially. In this case, the duration of particle oscillations increases and the amplitudes decrease. Thus, at $\bar{z} = 10$ (at a depth equal to the R-wave length), the duration

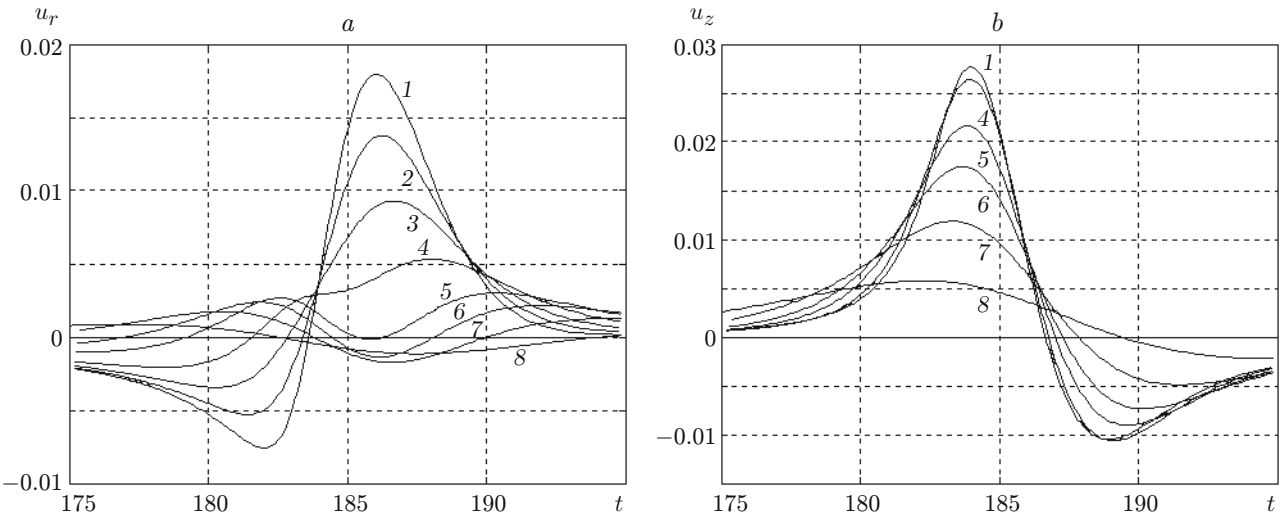

Fig. 2. Horizontal (a) and vertical (b) displacement components versus time ($r = 100$ and $z_0 = 1$) for $\bar{z} = 0$ (1), 0.2 (2), 0.5 (3), 1 (4), 2 (5), 3 (6), 5 (7), and 10 (8).

of the oscillations increases by a factor of approximately three compared to the duration of the oscillations on the free surface. The perturbation of the surface damps faster than that at the depth. The R-wave propagates in two directions: along the free surface and into the depth. The amplitude along the free surface attenuates as $r^{-1/2}$.

Figure 3 gives particle trajectories for the passage of the R-wave at various relative depths $\bar{z} = z/\lambda$. At $\bar{z} = 0$, the trajectories are close in shape to ellipses whose major axes are oriented along the z axis. The particles rotate counterclockwise. As the depth increases, the vertical component remains almost unchanged and the horizontal component decreases linearly. At $\bar{z} = 0.15$–0.20, the horizontal component decreases to zero, after which it changes sign and the rotation of the particles changes direction. At greater depths, they rotate clockwise. Thus, the surface wave divides the near-surface layer of the elastic medium into two sublayers, in which the particles rotate in different directions. At $\bar{z} > 0.20$, the amplitudes of both components decrease monotonically and rapidly. At a depth $\bar{z} = 1$, the modulus of the displacement vector is almost an order of magnitude smaller than that on the free surface.

Qualitatively, the particle motion in the blast R-wave is similar to the motion in a harmonic wave. The difference is that for the harmonic wave, the position of the boundary z_s on which the direction of particle rotation changes is defined by formula (3.1), whereas in the blast wave there is no distinct boundary is absent. The change of particle rotation occurs gradually in the neighborhood of the value z_s.

3.2. *Stresses.* Figure 4 gives curves of the stress amplitudes versus the reduced depth for the stress tensor components σ_{ik}, the shear stress intensity $\tau_i = \sqrt{(\sigma_{rr} - \sigma_{\varphi\varphi})^2 + (\sigma_{\varphi\varphi} - \sigma_{zz})^2 + (\sigma_{zz} - \sigma_{rr})^2 + 6\sigma_{rz}^2}/3$, and the mean stress $p = (\sigma_{rr} + \sigma_{\varphi\varphi} + \sigma_{zz})/3$. From Fig. 4 it follows that the amplitudes of the stresses σ_{rr}, $\sigma_{\varphi\varphi}$, τ_i, and p have the largest values on the free surface and decrease monotonically as the depth increases. The amplitudes of σ_{zz} and σ_{rz} reach the largest value at approximately the same depth at which there is a change in the direction of particle rotation. The dependence $\tau_i(z)$ is more complex and has two extrema: a minimum near the free surface and a maximum at $z \approx z_s$.

Figure 5 shows curves of $\tau_i(t)$ and $p(t)$ for various reduced depths. In Fig. 5b, it is evident that the dependence $p(t)$ have three characteristic segments. When the R-wave arrives, the medium is extended on the first segment, is compressed on the second segment, and is extended again on the third segment. The shear stress intensity varies in synchrony with the variation in the mean stress. At the times the mean stresses reach extrema, the shear stress intensity is also extremal. As the depth increases, the stress decreases rapidly. For example, at $\bar{z} = 5$, i.e., at a depth equal to half the wavelength, the mean stress is approximately two orders of magnitude lower than that on the free surface and τ_i decreases by a factor of nearly five.

From the calculations results, it follows that the dependences given above are qualitatively similar to the dependences obtained for different values of γ ($0 < \gamma < 1/\sqrt{2}$).

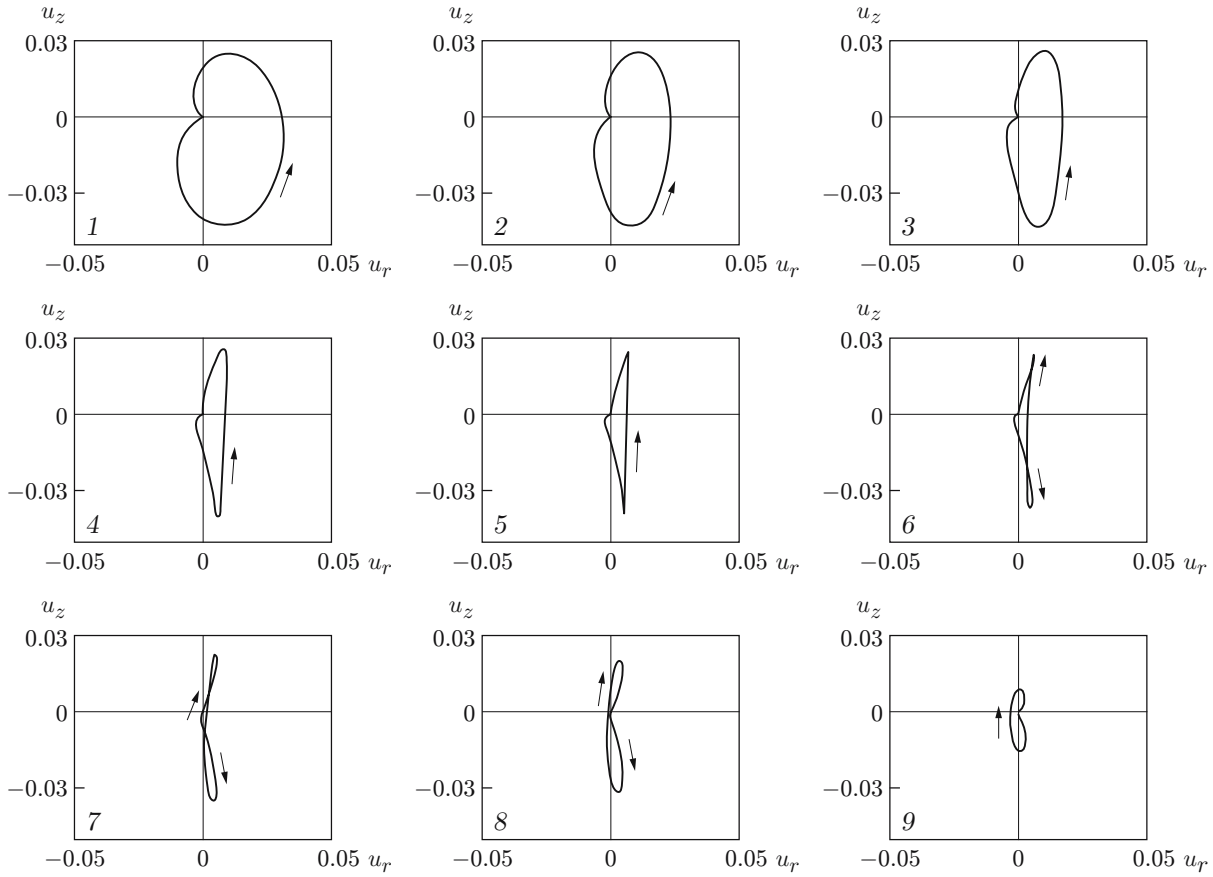

Fig. 3. Particle trajectories in the R-wave ($r = 100$) for $\bar{z} = 0$ (1). 0.02 (2), 0.04 (3), 0.08 (4), 0.10 (5), 0.12 (6), 0.15 (7), 0.20 (8), and 0.50 (9); the arrows show the direction of particle rotation.

4. Energy of the Blast Rayleigh Wave. The Rayleigh wave is formed at a certain some distance from the epicenter of the explosion. Its formation and separation from the body-wave train occurs at a distance from the epicenter equal to several wavelengths.

To find the explosion energy transferred to the R-wave, we consider the energy flux through a control surface area S that bounds the explosion site and at a distance $r \geqslant 3\lambda \approx 30$ from the epicenter. As such a surface, it is convenient to use the surface of a semi-infinite round cylinder of radius $r = R_0$ whose symmetry axis coincides with the z axis and whose upper end coincides with the free surface. The rate of change in the energy contained in the R-wave is equal to the energy flux through the surface S:

$$\frac{dE_R}{dt} = -\int\limits_S \boldsymbol{P}\cdot\boldsymbol{n}\,dS = -\int\limits_{S_s} \boldsymbol{P}\cdot\boldsymbol{n}\,dS - \int\limits_{S_u} \boldsymbol{P}\cdot\boldsymbol{n}\,dS - \int\limits_{S_d} \boldsymbol{P}\cdot\boldsymbol{n}\,dS.$$

Here S_s is the lateral area of the cylinder, S_u and S_d are the surface areas of the top and bottom ends, respectively, $P_i = \sigma_{ik}v_k$ are the components of the Umov–Poynting vector, and $\boldsymbol{n}$ is the normal vector to the surface S.

The integral over S_u is equal to zero by virtue of the boundary conditions on the free surface, and the integral over S_d tends asymptotically to zero by virtue of the exponential decay of the motion in the R-wave at great depths. The integral over S_s can be written as

$$\frac{dE_R}{dt} = -2\pi R_0 \int\limits_0^\infty (\sigma_{rr}v_r + \sigma_{zz}v_z)\Big|_{r=R_0}\,dz = -2\pi R_0\Big(\varepsilon(t-t_p)\int\limits_0^{z_p}(\sigma^\varphi_{rr}v^\varphi_r + \sigma^\varphi_{rz}v^\varphi_z)\Big|_{r=R_0}\,dz$$

$$+\,\varepsilon(t-t_s)\int\limits_0^{z_s}\Big[(\sigma^\varphi_{rr}v^\psi_r + \sigma^\psi_{rr}v^\varphi_r + \sigma^\psi_{rr}v^\psi_r) + (\sigma^\varphi_{rz}v^\psi_z + \sigma^\psi_{rz}v^\varphi_z + \sigma^\psi_{rz}v^\psi_z)\Big]\Big|_{r=R_0}\,dz\Big). \tag{4.1}$$

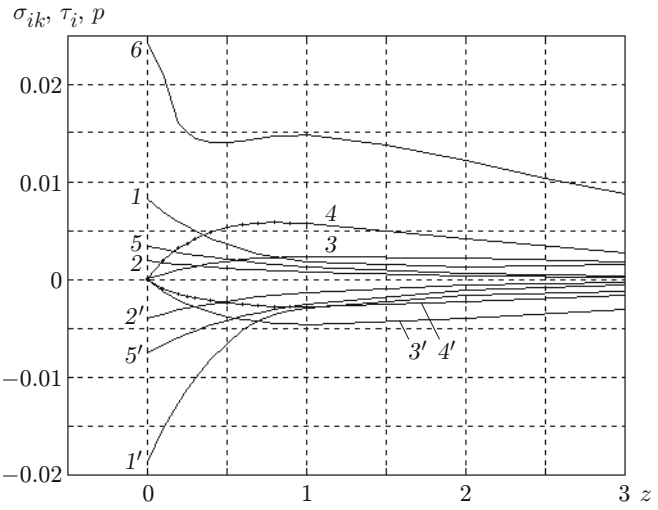

Fig. 4. Stress amplitudes versus the reduced depth ($r = 100$): σ_{rr} (1 and 1′), $\sigma_{\varphi\varphi}$ (2 and 2′), σ_{zz} (3, 3′), σ_{rz} (4 and 4′), p (5 and 5′), and τ_i (6); curves 1–6 refer to the phases with a positive amplitude and curves 1′–5′ refer to the phases with a negative amplitude.

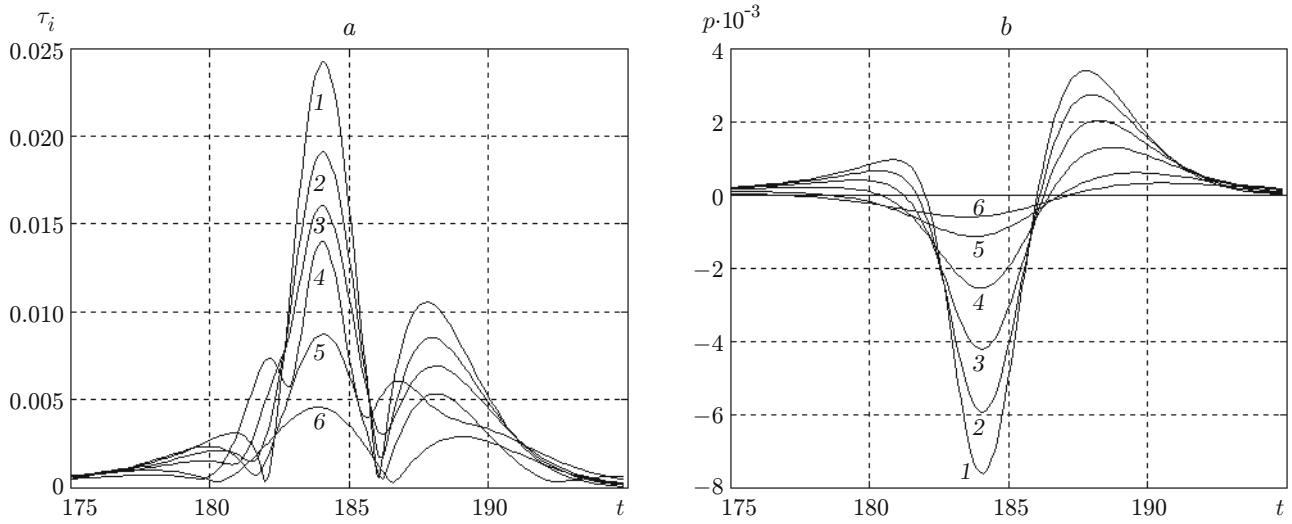

Fig. 5. Shear stress intensity τ_i (a) and the mean stress p (b) for $r = 100$ and $\bar{z} = 0$ (1), 0.1 (2), 0.2 (3), 0.5 (4), 3 (5), and 5 (6).

Here the upper limits of integration z_p and z_s are the coordinates of the point of intersection of the fronts of the reflected PP- and PS-waves with the generatrix of the cylinder $r = R_0$ (see Fig. 1). For the specified time t, we have $z_p = \sqrt{t^2 - R_0^2} - z_0$, and the value of z_s is found by solving the system of equations

$$\sqrt{z_0^2 + C^2} + \sqrt{(R_0 - C)^2 + z_s^2}/\gamma = t,$$

$$(R_0 - C)\sqrt{z_0^2 + C^2} - \gamma C\sqrt{(R_0 - C)^2 + z_s^2} = 0.$$

The energy concentrated in the Rayleigh wave is obtained by integrating expression (4.1) over time:

$$E_R = -\int_0^\infty \int_S \boldsymbol{P} \cdot \boldsymbol{n}\, dS\, dt = \varkappa^2 (c_p t_0)^3 \rho c_p^2 \varepsilon_R \tag{4.2}$$

TABLE 2

z_0	E_R	B	E_p/E_0, %	E_R/E_p, %	E_R/E_0, %
1.0	0.500	0.21	8.75	10.0	0.880
2.0	0.230	0.20	7.70	5.0	0.380
3.0	0.145	0.18	7.20	3.6	0.260
4.4	0.095	0.17	6.50	2.4	0.160
5.0	0.085	0.16	6.30	2.3	0.145
10.0	0.037	0.11	4.45	2.2	0.076
14.4	0.0245	0.06	3.25	2.1	0.700

(ε_R is the R-wave energy in dimensionless form). It should be noted that the value of ε_R does not depend on the radius R_0 of the control cylinder. Using (4.2) and (1.2), we obtain

$$\frac{E_R}{E_0} = \frac{E_p \varepsilon_R}{E_0 \pi \alpha(B)}.$$

The energy concentrated in the Rayleigh wave depends on the depth of the source, which in the calculations was varied in the range of $z_0 \in (1; 14.4)$. The value $z_0 = 1$ is close to the contained-explosion depth. An explosion at a depth $z_0 \leqslant 1$ produces spalls of the ground. In this case, the elastic model is inappropriate.

To calculate the energy of the R-wave by formula (4.2), one needs to know the dependences of the energy of the P-wave and the parameter B in the expression for the source function (1.1) on the charge depth. For rock salt at $z_0 = 4.4$ and 14.4, they can be found from experimental data on the Gnome and Salmon explosions (see Table 1), which were approximated by a linear dependence on z_0 for B and an exponential dependence on z_0 for $\eta = E_p/E_0$:

$$B = 0.22 - 0.011 z_0, \qquad \eta = 0.088 \exp(-0.0695 z_0), \qquad 1 \leqslant z_0 \leqslant 14.4. \tag{4.3}$$

The expression for η was chosen such that it yielded the average values of η given in Table 1.

The results of calculations using relation (4.3) are given in Table 2 (the calculations were performed for a control cylinder of radius $R_0 = 100$). The fourth and seventh columns ($z_0 = 4.4$ and 14.4) give data obtained for the Gnome and Salmon explosions, respectively. From Table 2 it follows that for $z_0 \approx 1$, about 1% of the explosion energy is converted to the R-wave energy. As the explosion depth increases, the fraction of the energy transferred to the R-wave decreases. The minimum charge depth at which the explosion can still be considered a contained one is $\bar{h} = 30$ m/kton$^{1/3}$ [20]. An extrapolation of the data of Table 2 to this depth shows that the energy expended in the formation of the R-wave is about 30% of the energy of the P-wave or approximately 3% of the explosion energy.

The energy of the R-wave was also estimated for the case of an explosion in granite using the data of the Hardhat U.S. test (1962). The energy of this explosion was $q = 5$ ktons [20]. The value of $B = 0.24$ is taken from [11], and $c_p t_0 = 68$ m/kton$^{1/3}$ from [20]. In this case, $z_0 = 4.42$ and $\gamma = 0.6$. The fraction of the energy transferred to the R-wave was about 0.5%.

It should be noted that for shallow charge depths, at which spalling and ground excavation occur, the procedure described above provides only estimates for the R-wave energy. For such depth, it is necessary to use more accurate expressions for the source function than relation (1.1).

Conclusions. The solution obtained describes the motion of material in seismic Rayleigh waves produced by explosions both on the surface and in the bulk. Trends in the variation of the displacements and stresses with depth and their dependences on the explosion yield and depth were obtained. The fraction of the energy that passes into the Rayleigh wave during explosion was determined. It can be considerable (up to several percent) for near-surface explosions in rocks. For explosions at greater depths, this fraction decreases almost linearly as the depth increases.

The solution obtained is useful for the estimation of the seismic effect on engineering facilities from strong explosions and high-velocity impacts of cosmic bodies on the Earth. In addition, it provides a more accurate description of the fracture pattern and the formation of explosion pipes in the antipode regions under impacts of cosmic bodies on the surface of solid planets.

REFERENCES

1. Lord Rayleigh (J. W. Strut), "On waves propagated along the plane surface of an elastic solid," *Proc. London Math. Soc.*, **17**, 4–11 (1885).
2. K. Aki, M. Bouchon, and P. Reasenberg, "Seismic source function for an underground nuclear explosion," *Bull. Seismol. Soc. Amer.*, **64**, No. 1, 131–148 (1974).
3. V. A. Simoneneko and N. I. Shishkin, "Cumulation of seismic waves during formation of kimberlite pipes," *J. Appl. Mech. Tech. Phys.*, **44**, No. 6, 760–769 (2003).
4. H. Nakano, "On Rayleigh waves," *Jpn. J. Astron. Geophys.*, **2**, 233 (1925).
5. E. R. Lapwood, "The disturbance due to a line source in a semi-infinite elastic medium," *Philos. Trans. Roy. Soc. London*, **A242**, 63 (1949).
6. K. I. Ogurtsov and G. I. Petrashen', "Dynamic problems for an elastic half-space in the case of axial symmetry," *Uch. Zap. Leningrad. Univ., Ser. Mat.*, **149**, No. 24, 3–117 (1951).
7. G. I. Petrashen', "Methods for studying wave processes in media containing spherical or cylindrical interfaces," *Uch. Zap. Leningrad. Univ.*, **170**, No. 3, 96–220, (1953).
8. N. I. Onis'ko and E. I. Shemyakin, "Motion of the free surface of a homogeneous ground in an underground explosion," *Prikl. Mekh. Tekh. Fiz.*, No. 4, 82–93 (1961).
9. Z. Alterman and F. Abramovici, "Effect of the depth of a point source on the motion of the surface of an elastic solid sphere," *Geophys. J. Roy. Astron. Soc.*, **11**, 189–224 (1966).
10. L. M. Brekhovskikh, "On the surface waves in solids confined by the curvature of the boundary," *Akust. Zh.*, **13**, No. 4, 541 (1967).
11. N. A. Haskell, "Analytic approximation for the elastic radiation from a contained underground explosion," *J. Geophys. Res.*, **76**, No. 10, 2583–2587 (1967).
12. D. Von Seggern and R. Blandford, "Source time functions and spectra for underground nuclear explosions," *Geophys. J. Roy. Astron. Soc.*, **31**, Nos. 1/3, 83–98 (1972).
13. N. I. Shishkin, "On the problem of disintegration of rock by an explosion under the influence of a free surface," *J. Appl. Mech. Tech.*, **3**, 401–408 (1981).
14. A. I. Shakhov and N. I. Shishkin, "On the problem of a confined explosion in an elastic half-space," *J. Appl. Mech. Tech.*, **38**, No. 5, 655–665 (1997).
15. D. W. Patterson, "Nuclear decoupling, full and partial," *J. Geophys. Res.*, **71**, No. 14, 3427–3436 (1966).
16. W. D. Werth, "Particle motion near a nuclear detonation in halite," *Bull. Seismol. Soc. Amer.*, **52**, No. 5, 981–1005 (1962).
17. G. C. Werth and R. F. Werth, "Comparison of amplitudes of seismic waves from nuclear explosions in four mediums," *J. Geophys. Res.*, **68**, 1463 (1963).
18. G. Werth and P. Randolph, "The Salmon seismic experiment," *J. Geophys. Res.*, **71**, No. 14, 3405–3413 (1966).
19. H. Healy, Chi-Yu King, O'Neill, "Source parameters of the Salmon and Sterling nuclear explosions from seismic measurements," *J. Geophys. Res.*, **76**, No. 14, 3335–3344 (1971).
20. H. Rodean, *Nuclear Explosion Seismology*, Atomic Energy Commission, Washington (1971).